Aerosol and Air Quality Research, 11: 664–678, 2011

ISSN: 1680-8584 print / 2071-1409 online
doi: 10.4209/aaqr.2010.12.0113

Physicochemical Properties of $PM_{2.5}$ and $PM_{2.5–10}$ at Inland and Offshore Sites over Southeastern Coastal Region of Taiwan Strait

Hsieh-Hung Tsai[1], Chung-Shin Yuan[1*], Chung-Hsuang Hung[2], Chitsan Lin[3]

[1] *Institute of Environmental Engineering, National Sun Yat-Sen University, Kaohsiung, Taiwan*
[2] *Department of Safety, Health and Environmental Engineering, National Kaohsiung First University of Science and Technology, Kaohsiung, Taiwan*
[3] *Department of Marine Environmental Engineering, National Kaohsiung Marine University, Kaohsiung, Taiwan*

ABSTRACT

This study investigates the effects of sea-land breezes (SLBs) and northeastern monsoon (NEM) on the physicochemical properties of particulate matter (PM) in the atmosphere over southeastern coastal region of Taiwan Strait. The intensive PM sampling protocol was consecutively conducted for forty-eight hours. During the sampling periods, $PM_{2.5}$ and $PM_{2.5–10}$ were simultaneously measured with dichotomous samplers at four sites (two inland and two at offshore sites) and PM_{10} was measured with beta-ray monitors at these same four sites. Strong SLBs were regularly observed in the coastal region of southern Taiwan during the SLBs periods, while significant northeastern monsoons appeared during the NEM periods. The mass ratios of $PM_{2.5}/PM_{10}$ during the NEM periods were always higher than the SLBs periods. The most abundant ionic species of PM were SO_4^{2-}, NO_3^-, and NH_4^+. The most common chemical compounds of PM in southern Taiwan were ammonium sulfate ($(NH_4)_2SO_4$) and ammonium nitrate (NH_4NO_3). Carbon contents of PM during the NEM periods were higher than during the SLBs periods. The organic-to-elemental-carbon ratio (OC/EC) of $PM_{2.5}$ ranged from 1.05 to 4.39 with an average of 2.26. The order of major metallic elements of $PM_{2.5}$ in the SLBs and NEM periods is Fe > Ca > K > Al > Mg > Zn > Pb and Ca > Fe > Al > K > Mg > V > Ni, respectively, and of $PM_{2.5–10}$ is Ca > K > Al > Fe > Mg > Zn and Fe > Ca > Al > K > Mg > V > Ni, respectively. This study reveals that the accumulation of PM offshore, due to land breezes, influences the tempospatial distribution of PM at the coastal region in southern Taiwan. Moreover, the nss-$[SO_4^{2-}]/[Na^+]$ ratio regarded as a PM pollution index, is more suitable than the $[NO_3^-]/[Na^+]$ ratio.

Keywords: Coastal region; Particulate matter; Sampling and analysis; Physicochemical properties; Backward trajectory.

INTRODUCTION

Atmospheric particulate matter (PM) is a complex mixture of elemental carbon (EC), organic carbon (OC), ammonium (NH_4^+), nitrates (NO_3^-), sulfates (SO_4^{2-}), mineral trace elements, and water (Turnbull and Harrison, 2000; Lee and Kang, 2001; Lin, 2002; Hueglin *et al*., 2005). Among them, SO_4^{2-}, NO_3^- and NH_4^+ are the most abundant components of atmospheric PM in the atmosphere. NO_3^- may be present in the gas phase as nitric acid vapor, however, SO_4^{2-} is almost exclusively found in the particle phase (Wyers and Duyzer, 1997). Organic carbon (OC) and elemental carbon (EC) particles are released mainly from incomplete combustion of carbonaceous fuels. EC is essentially a primary pollutant, emitted directly from the combustion processes, while OC has both primary and secondary origins. Primary OC is emitted in particulate form, while secondary OC is formed in the atmosphere through the gas-to-particle conversion processes of volatile organic compounds (VOCs) (Pandis *et al*., 1992; Pankow, 1994).

Sea-land breezes (SLBs) and northeastern monsoon (NEM) play important roles in transporting air pollutants to and from urban area at the coastline in southern Taiwan (Ding *et al*., 2004; Tsai *et al*., 2008). Several studies have analyzed air mass quality and meteorological datasets in order to interpret atmospheric aerosol levels in European and Asian cities (Hien *et al*., 2002; Yang, 2002; Oanh *et al*., 2006). Smith *et al*. (2001) used 3-year PM_{10} data sets from three monitoring sites, in combination with relevant air trajectory and meteorological data, to identify factors influencing particulate matter levels in Greater London. Previous researches have investigated the effects of SLBs on the spatial distribution and transport of ambient air pollutants, particularly for ozone episodes (Nester, 1995; Venkatesan *et al*., 2002; Ding *et al*., 2004; Levin *et al*., 2005; Evtyugina *et al*., 2006; Tsai *et al*., 2008). Only a few

* Corresponding author. Tel.: 886-7-5252000 ext 4409; Fax: 886-7-5254449
E-mail address: ycsngi@mail.nsysu.edu.tw

investigations have focused on the influence of SLBs on atmospheric aerosols (Rodríguez *et al*., 2002; Viana *et al*., 2005). Their studies investigated about the origin of high PM_{10} and TSP concentrations at coastal sites in eastern Spain. Atmospheric coastal dynamics can exert a significant influence on the levels and chemical composition of atmospheric PM (Viana *et al*., 2005). Sea breezes may penetrate deep inland and cause ozone episodes by early afternoon, resulting in higher concentration of marine aerosols in the daytime than in the nighttime (Ding *et al*., 2004). Sea-salt particles are important in both the chemistry and radiative transfer occurring in the lower troposphere (O'Dowd *et al*., 1997). Moreover, Levin *et al*. (2005) revealed that land breezes over a lake in the nighttime bring newly emitted particulate matter to the southeast of the Dead Sea, which is responsible for the formation of lower haze layer in the early morning.

High PM_{10} episodes frequently occur over southern Taiwan, a highly industrialized region (Tsai *et al*., 2010). In the fall, shallow northeasterly winds prevail after a frontal passage and are diverted by the Central Mountain Ridge because of its mean altitude of about 2,600 m. Numerical results indicate that anthropogenic emissions from the north of metro Kaohsiung contribute as much as 41% of ozone to the metro Kaohsiung and 24% to the inland rural area during the northerly flow (Lin *et al*., 2007). After a sea breeze develops, strong onshore flows transport significant amounts of air masses with preformed ozone and/or its precursors to the inland rural areas, resulting in high ozone episodes that frequently occur over southern Taiwan during the fall season. Both numerical and field sampling studies have investigated on the air-pollution episodes in northern, central, southwestern, and southern Taiwan (Cheng, 2002; Yu and Chang, 2000; Liu *et al*., 2002; Tsai and Chen, 2006). These investigations mainly focused on the origin of ozone and the influence of SLBs on the tempospatial distribution of ozone during the O_3 episodes. However, no investigation has been conducted to study the effects of SLBs on the physicochemical properties of PM during the PM_{10} episodes in southern Taiwan.

Previous researches have investigated about the seasonal and spatial distribution of ambient air pollutants by using field measurement data obtained from the inland stations of Taiwan Air Quality Monitoring Network (TAQMN) of Taiwan Environmental Protection Administration (TEPA). So far, offshore sampling of air pollutants has not been carried out in southern Taiwan. A previous study has revealed that PM has a tendency to be transported back and forth across the coastline of southern Taiwan during the PM_{10} episodes (Tsai *et al*., 2010). Moreover, the accumulation of air pollutants in the offshore region due to SLBs might cause local hot spots in the highly polluted region.

DATA COLLECTION AND METHODS

Sampling Protocol

In this study, particulate matter was simultaneously collected both inland and offshore during five sampling periods: August 16–18 (I), November 2–4 (II), 2006, January 24–26 (III), March 6–8 (IV), and May 2–4 (V), 2007. Inland sampling was conducted at two sites associated with fourteen stations of TAQMN, while offshore sampling was conducted at Hsiau-Liou-Chiou Island (HLC) (approximately 14 km offshore) and on a mobile air quality monitoring boat. The sampling periods (I) (II) (V) were selected to investigate the influence of SLBs on the spatial and temporal variation of PM in the summer season, while the sampling periods (III) (IV) were selected to investigate the influences of both SLBs and NEM on the spatial and temporal variation of PM in the winter season. The location of the inland and offshore sites over southeastern coastal region of Taiwan Strait is shown in Fig. 1.

Inland PM sampling was conducted at fourteen sites, including twelve stations of TAQMN and two others selected for this particular study. The two sites during the SLBs periods were located at the National Kaohsiung University (NKU; 22.732°N, 120.285°E) and Fu-In College (FIC; 22.604°N, 120.390°E), while the three sites for the NEM period were located at the Zao-In Junior High School (ZIJ; 22.678°N, 120.295°E), Chi-Shen Junior High School (CSJ; 22.631°N, 120.287°E), and National Kaohsiung First University (NKFU; 22.758°N, 120.337°E). At these sampling sites, mobile air quality monitoring vehicles were used to simultaneously collect atmospheric PM ($PM_{2.5}$, $PM_{2.5–10}$, and PM_{10}) with dichotomous samplers (Anderson, Model Series 241). The sampling flow rate of the dichotomous sampler was 16.7 L/min, and the filters used in this study were 37 mm quartz filter. Offshore PM sampling was conducted at two sites located in the Taiwan Strait, including an offshore island, Hsiau-Liu-Chiou (HLC; 22.350°N, 120.368°E), approximately 14 km away from the southwest coast of Kaohsiung City, and a mobile air quality monitoring boat navigated about 4–12 kilometers away from the coastline of Kaohsiung City. Atmospheric PM mixed with marine aerosols ($PM_{2.5}$, $PM_{2.5–10}$, and PM_{10}) were sampled at the top of the boat with a dichotomous sampler to prevent the interferences from the exhaust gases of the boat itself as well as the seawater sprays emitted from the ocean. The routes of the boat were along the coast of southern Taiwan for offshore sampling of marine aerosols during the five sampling periods.

In order to investigate the influence of SLBs and NEM on the tempo-spatial distribution of atmospheric PM, a PM sampling protocol was consecutively conducted for forty-eight hours (from 8:00 am to 8:00 am) in each sampling period. During the sampling periods, $PM_{2.5}$ and $PM_{2.5–10}$ were collected by a dichotomous sampler at each sampling site. PM_{10} was measured by dichotomous samplers at four sites (including inland and offshore sites) and β-ray monitors at twelve ambient stations of TAQMN. Offshore PM sampling on the boat having traveled along the coast of southern Taiwan was conducted to collect marine aerosols by a dichotomous sampler and a β-ray monitor during the sampling periods. Quartz filters of 37 mm were used to collect atmospheric aerosols for further analysis of their chemical composition.

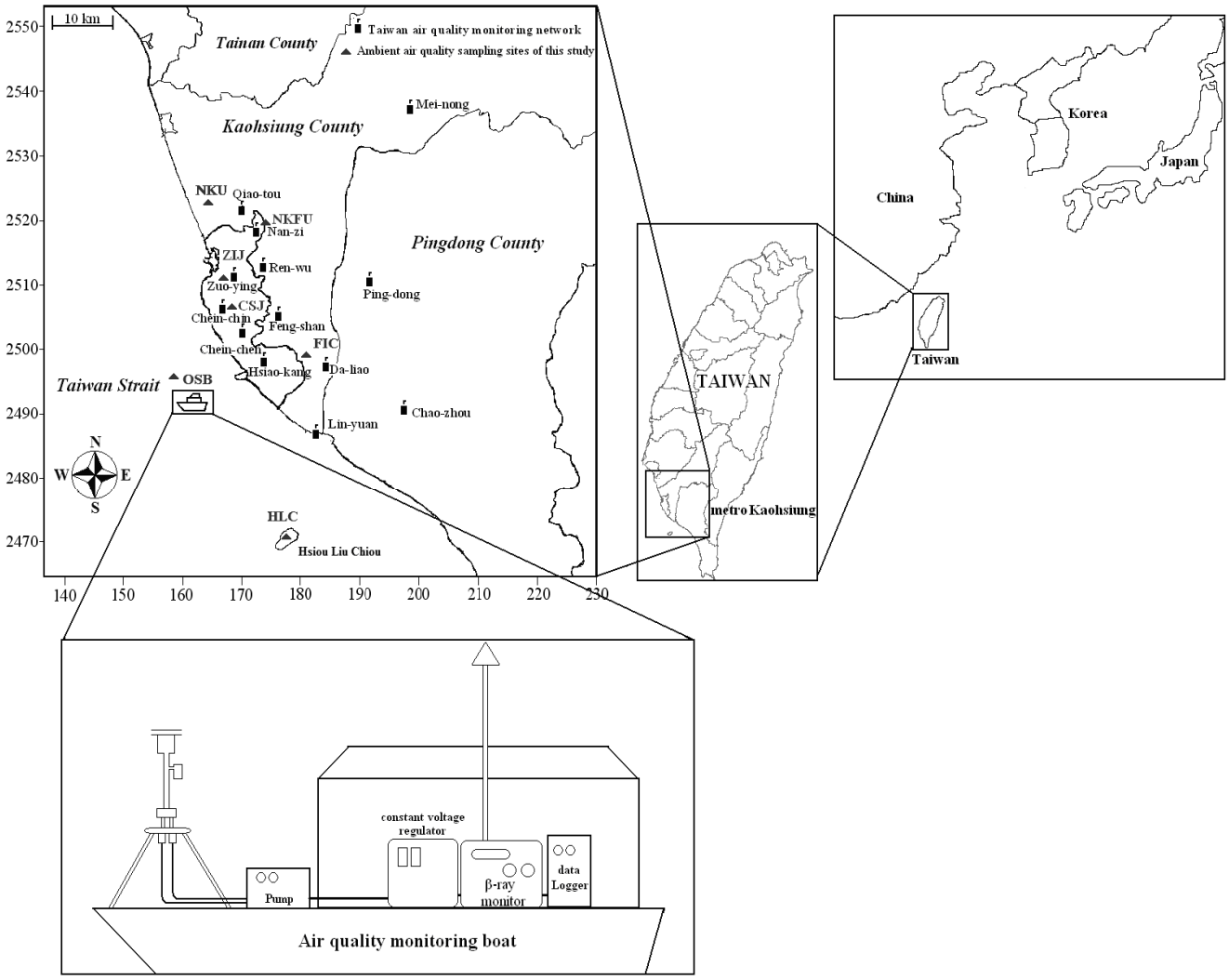

Fig. 1. Location of the PM sampling sites around the coastal region of southern Taiwan and the mobile air quality monitoring boat for the offshore monitoring protocol(x- and y-axis legends are UTM in kilometer).

Chemical Analysis

After sampling, quartz filters were temporarily stored at 4°C and transported back to the Air Pollution Laboratory in the Institute of Environmental Engineering at the National Sun Yat-Sen University for further conditioning, weighing, and chemical analysis. The quartz filters were initially cut into four identical parts. One part was analyzed for ionic species, two parts were used for the analysis of carbonaceous content, and the rest was used for analysis of metallic content. The filters for ionic species were put into 15-mL PE bottles. Distilled, de-ionized water was added into each bottle prior to ultrasonic process for approximately 60 min. Ion chromatography (DIONEX DX-120) was used to analyze major anions (F^-, Cl^-, SO_4^{2-}, and NO_3^-) and cations (NH_4^+, Ca^{2+}, Na^+, K^+, and Mg^{2+}) (Yuan *et al.*, 2004). A quarter of the filter analyzed for metals was digested in 20 mL concentrated nitric acid at 150–200°C for 2 h, and then diluted to 25 mL with distilled de-ionized water (D.I. H_2O). For the analysis of metallic content, the filters were initially digested in a 30 mL mixed acid solution (HNO_3:$HClO_4$ = 3:7). During the digestion, D.I. H_2O was added into the residual solution twice or more in order to eliminate the acid content of the digestion solution. The residual solution was then diluted to 25 mL using 0.5 N HNO_3 and stored in PE bottles. The metallic elements of PM included Ti, As, Fe, Cu, Mn, Ca, Mg, K, Al, Pb, Cd, Ni, Cr, Zn, and V, and were further analyzed with an inductively coupled plasma-atomic emission spectrometer, ICP-AES (Perkin Elmer, Optima 2000DV). Moreover, total and elemental carbons (TC and EC) of PM were determined with an elemental analyzer, EA (Carlo Erba EA 1108). A quarter of each filter was heated in an oxygen-free environment at 340°C for 100 min to expel OC and then fed into the elemental analyzer to obtain the EC content. Another quarter of each filter was fed directly into the elemental analyzer without pre-heating to obtain the TC content (Lin, 2002). OC could then be determined by subtracting EC from total carbons TC.

Backward Trajectory

Backward trajectories were simulated with an Air Quality Trajectory Model (version 1.1) developed by Taiwan EPA.

The assimilation method, which incorporates Barnes objective method to interpolate spatial values and the variation-kinematical model, was adopted to correct the effects of complex terrain and produce the hourly wind fields data by using 24 surface stations over southern Taiwan, including two meteorological stations from the Central Weather Bureau of Taiwan (CWBT) and 22 ambient air quality monitoring stations from the Taiwan Air Quality Monitoring Network (TAQMN). By utilizing the hourly wind fields over surface, backward trajectories were simulated for 10 h initiating at seven selected air quality monitoring stations. The trajectories were constructed using only the horizontal wind components, had a segment resolution of 1 h, and the interpolation was linear in both time and space. The initial time of backward trajectories for each monitoring station was set whenas the maximum hourly PM_{10} concentration was observed.

Quality Assurance and Quality Control

The quality assurance and quality control (QA/QC) for both PM sampling and chemical analysis were conducted in this study. Prior to conducting PM sampling, the sampling flow rate of each PM sampler was carefully calibrated with a film flowmeter (MCH-01 SENSIDYNE Inc.). Both field and transportation blanks were conducted for PM sampling, while reagent and filter blanks were undertaken for chemical analysis. The determination coefficient (R^2) of the calibration curve for each chemical species was required to be higher than 0.995.

RESULTS AND DISCUSSION

Meteorological Data

In this study, we observed the diurnal variation of meteorological parameters around the coastal region of southern Taiwan during the intensive sampling periods (Table 1). Three sampling periods (I) and (V) were influenced by SLBs, while two other periods (III) and (IV) were dominated by NEM. During the sampling period (I), sea breezes from directions of 300°–350° blew at 10:00–23:00, while land breezes (2–4 m/sec) were regularly observed at nighttime. The sampling period (II) was influenced by both SLBs and NEM blown in the directions of 300°–350° and 250°–40°, respectively. The sampling periods (III) and (IV) with typical winter weather were dominated by NEM, whereas the winds were blown in the directions of 300°–30° with wind speeds of 2–6 m/sec.

Taiwan, located in the East Asian subtropical region, is predominantly influenced by the northeasterly monsoon from late fall to spring and by the southwesterly monsoon from summer to mid-fall. Sea breezes are superimposed on these monsoons when meteorological conditions are suitable for producing a daytime northwesterly or southwesterly flow. The surface flows are generally weak, but increase in speed from almost calm up to about 2 m/sec and remain steady for 5–6 hours throughout the afternoon, with wind directions between 270° and 300°. Similar results were found by Kambezidis *et al*. (1998). They found that the summer southwesterly flows showed stronger sea breezes, with the wind speeds increasing from < 2 to 4 m/sec and the directions of southwesterly flow confined to the sector 200°–270° (Kambezidis *et al*., 1998). Air temperature contrasts between the land and the sea drive sea breezes when the land is strongly heated under cloudless skies and calm conditions (Byun *et al*., 2007). Strong land breezes were regularly observed at nighttime during the monitoring periods (I), (II), and (V), respectively. However, no significant SLBs appeared in the coastal region of southern Taiwan during the sampling periods (III) and (IV).

PM Concentration

The concentration of $PM_{2.5}$, $PM_{2.5–10}$, and PM_{10} collected at the seven selected sampling sites is summarized in Table 1. Atmospheric PM levels at the inland sites (NKU and FIC) were generally higher than those at the offshore sites (OSB and HLC) since industrial and mobile sources in the inland region were the major particle emission sources during the SLBs periods (Table 2). The daytime concentrations of $PM_{2.5}$ and $PM_{2.5–10}$ at the inland sites were higher than those at nighttime except for the OSB sites. Moreover, the averaged mass ratios of $PM_{2.5}$ to PM_{10} ($PM_{2.5}/PM_{10}$) at the inland sites were higher than those at the offshore sites. These results concurred with previous researches, indicating that PM concentration is relatively lower during the land breeze periods than during the sea breeze periods (Tsai *et al*., 2008). The highest PM_{10} level up to 90.79 ± 41.12 μg/m^3 was observed in daytime at NKU where it had been previously claimed, incorrectly, as having the best air quality zone in metro Kaohsiung. The $PM_{2.5}/PM_{10}$ ratios observed at the inland sites ranged from 53.14% to 57.36% with an average of 55.09%, while the $PM_{2.5}/PM_{10}$ ratio at the offshore sites ranged from 45.36% to 49.73% with an average of 47.38%. These results indicated that the inland sites had a higher fraction of fine

Table 1. Meteorological parameters measured during the intensive air quality monitoring periods.

Sampling Number	Sampling Periods	Wind Direction (Time)	Wind Speed (m/sec)	Weather Patterns
1	Aug. 16–18, 2006	Sea breeze: 300°–350° (10:00–23:00) Land breeze: 330°–60° (23:00–10:00)	1–4 2–4	SLBs
2	Nov. 2–4, 2006	270°–30°, 0°–60°	1–3	SLBs + NEM
3	Jan. 24–26, 2007	300°–30°	2–5	NEM
4	Mar. 6–8, 2007	300°–40°	2–6	NEM
5	May 2–4, 2007	Sea breeze: 240°–330° (09:00–21:00) Land breeze: 330°–60° (21:00–09:00)	1–5 1–5	SLBs

Table 2. The mass concentration and the ratios of different fraction of PM in the coastal region of southern Taiwan during the SLBs and NEM periods.

Sampling Sites/Periods		No. of samples	$PM_{2.5}$ (μg/m^3)	$PM_{2.5–10}$ (μg/m^3)	PM_{10} (μg/m^3)	$PM_{2.5}/PM_{10}$ (%)
[a]NKU	Daytime	n = 6	50.52 ± 21.78	40.27 ± 20.28	90.79 ± 41.12	55.7
	Nighttime	n = 6	36.05 ± 19.94	32.17 ± 18.58	68.21 ± 38.49	53.1
[a]FIC	Daytime	n = 6	43.89 ± 20.32	36.28 ± 14.58	80.17 ± 34.68	54.1
	Nighttime	n = 6	42.67 ± 26.26	29.63 ± 13.98	72.30 ± 38.84	57.4
[a]HLC	Daytime	n = 6	25.76 ± 6.42	29.79 ± 13.22	55.55 ± 19.48	47.5
	Nighttime	n = 6	26.97 ± 6.91	33.02 ± 10.82	60.00 ± 17.37	45.4
[a]OSB	Daytime	n = 6	34.97 ± 10.16	36.90 ± 17.59	71.87 ± 26.93	49.7
	Nighttime	n = 6	29.43 ± 8.35	33.68 ± 11.76	63.11 ± 20.10	47.0
[b]ZIJ	Daytime	n = 4	49.54 ± 12.64	19.21 ± 5.70	68.75 ± 17.16	72.2
	Nighttime	n = 4	60.99 ± 17.20	20.29 ± 12.11	81.28 ± 28.93	76.9
[b]CSJ	Daytime	n = 4	52.50 ± 7.91	31.75 ± 5.13	84.25 ± 11.54	62.3
	Nighttime	n = 4	58.25 ± 19.25	32.79 ± 12.10	91.04 ± 31.10	64.3
[b]NKFU	Daytime	n = 4	48.78 ± 11.65	31.99 ± 7.67	80.77 ± 19.32	60.4
	Nighttime	n = 4	58.07 ± 20.53	32.87 ± 13.84	90.93 ± 34.28	64.4
[b]OSB	Daytime	n = 4	53.71 ± 16.08	33.90 ± 5.67	87.61 ± 20.24	60.7
	Nighttime	n = 4	56.64 ± 29.19	40.15 ± 19.18	96.79 ± 48.34	58.0

[a] Sampling sites for the SLBs periods ; [b] Sampling sites for the NEM periods.

particles ($PM_{2.5}$), whereas the offshore sites had a higher fraction of coarse particles ($PM_{2.5–10}$). These phenomena were attributed to the fact that marine aerosols are generally abundant in the coarse particles (Yuan *et al*., 2004).

Table 1 also summarizes the average and standard deviation of PM concentrations at the inland and offshore sites during the NEM periods. The averaged concentrations of $PM_{2.5}$ and $PM_{2.5–10}$ at nighttime were higher than daytime at inland sites. Among four sites, ZIJ had the highest average $PM_{2.5}$ concentration (60.99 ± 17.20 μg/m^3) and OSB had the highest average PM_{10} concentration (96.79 ± 48.34 μg/m^3). During the NEM periods, the $PM_{2.5}/PM_{10}$ ratios at the inland sites were higher than the offshore sites. The concentrations in the fall and winter seasons with NEM were higher than those in the summer with SLBs in the coastal region, as illustrated in Fig. 2. The $PM_{2.5}/PM_{10}$ ratios during the NEM periods were always higher than those during the SLBs periods. During the NEM periods, the PM_{10} concentrations at the inland sites were higher than those at the offshore site. On the contrary, high PM_{10} concentrations observed during the NEM periods were mainly influenced by the northerly winds, which transported PM_{10} from the northern region to metro Kaohsiung.

Chemical Composition of PM

The ionic species, carbonaceous and metallic contents of $PM_{2.5}$ and $PM_{2.5–10}$ sampled in the coastal region of southern Taiwan during the sampling periods are summarized in Table 3. The most abundant chemical components of PM were SO_4^{2-}, NO_3^-, NH_4^+, and Cl^-. It indicated that the SO_4^{2-} concentration during the NEM periods was higher than that during the SLBs periods.

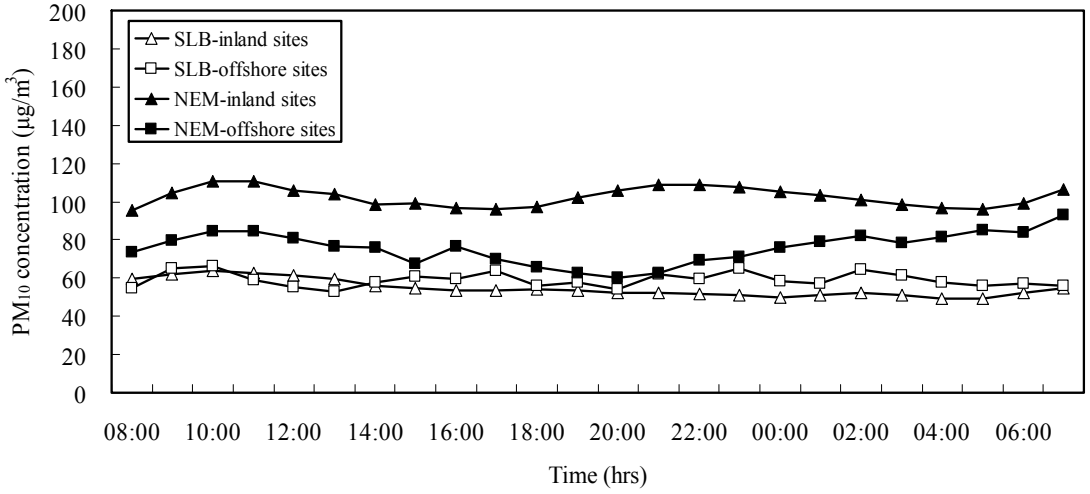

Fig. 2. Variation of PM_{10} concentration in the coastal region of southern Taiwan during the sampling periods.

Table 3. Ionic species, carbonaceous, and metallic contents of $PM_{2.5}$ and $PM_{2.5-10}$ sampled in the coastal region of southern Taiwan.

Chemical species	$PM_{2.5}$					$PM_{2.5-10}$			
	unit	SLBs-Inland	SLBs-Offshore	NEM-Inland	NEM-Offshore	SLBs-Inland	SLBs-Offshore	NEM-Inland	NEM-Offshore
Mass	$\mu g/m^3$	43.28 ± 19.83	29.29 ± 7.33	54.69 ± 14.02	55.17 ± 22.85	34.59 ± 13.87	33.35 ± 10.21	28.15 ± 10.72	37.02 ± 14.31
F^-	$\mu g/m^3$	0.05 ± 0.01	0.05 ± 0.04	0.03 ± 0.02	N.D.	0.08 ± 0.04	0.04 ± 0.03	0.02 ± 0.01	N.D.
Cl^-	$\mu g/m^3$	1.07 ± 0.27	1.96 ± 0.69	1.06 ± 0.27	3.11 ± 0.93	1.26 ± 0.32	2.34 ± 0.71	2.81 ± 0.83	5.68 ± 1.40
NO_3^-	$\mu g/m^3$	3.13 ± 1.79	2.18 ± 1.54	1.39 ± 0.45	2.84 ± 0.78	2.36 ± 1.20	1.49 ± 0.73	1.86 ± 0.65	1.52 ± 0.49
Br^-	$\mu g/m^3$	N.D.	N.D.	N.D.	N.D.	N.D.	N.D.	0.02 ± 0.01	0.03 ± 0.01
SO_4^{2-}	$\mu g/m^3$	5.02 ± 1.40	4.75 ± 0.63	13.21 ± 3.95	9.29 ± 2.20	3.86 ± 0.87	2.88 ± 0.63	3.08 ± 0.97	1.87 ± 0.44
Na^+	$\mu g/m^3$	0.58 ± 0.17	1.23 ± 0.44	0.76 ± 0.21	2.03 ± 0.61	0.65 ± 0.20	1.48 ± 0.44	1.97 ± 0.55	3.75 ± 0.94
NH_4^+	$\mu g/m^3$	2.12 ± 0.37	1.94 ± 0.72	4.21 ± 1.33	2.19 ± 0.65	1.10 ± 0.63	0.69 ± 0.27	0.99 ± 0.49	0.38 ± 0.03
K^+	$\mu g/m^3$	0.57 ± 0.23	0.63 ± 0.31	0.62 ± 0.17	0.83 ± 0.16	0.57 ± 0.29	0.50 ± 0.17	0.32 ± 0.10	0.27 ± 0.03
Mg^{2+}	$\mu g/m^3$	0.13 ± 0.04	0.19 ± 0.09	0.49 ± 0.18	0.50 ± 0.03	0.18 ± 0.05	0.22 ± 0.11	0.23 ± 0.09	0.19 ± 0.04
Ca^{2+}	$\mu g/m^3$	0.66 ± 0.30	0.56 ± 0.34	0.54 ± 0.14	0.80 ± 0.21	0.78 ± 0.30	0.55 ± 0.43	0.30 ± 0.07	0.23 ± 0.02
OC	$\mu g/m^3$	2.93 ± 1.49	2.15 ± 0.96	4.43 ± 1.32	3.15 ± 1.77	2.57 ± 1.38	2.71 ± 1.71	2.09 ± 0.89	1.94 ± 0.69
EC	$\mu g/m^3$	1.15 ± 0.61	1.64 ± 0.49	1.52 ± 0.40	1.67 ± 0.70	0.93 ± 0.50	1.90 ± 0.65	0.74 ± 0.32	1.36 ± 0.39
TC	$\mu g/m^3$	4.08 ± 2.08	3.79 ± 1.42	5.96 ± 1.68	4.81 ± 2.45	3.50 ± 1.86	4.61 ± 2.33	2.83 ± 1.21	3.30 ± 1.06
Ti	ng/m^3	35.19 ± 26.92	27.38 ± 18.51	12.26 ± 0.08	12.43 ± 0.20	25.88 ± 11.98	25.68 ± 13.98	11.50 ± 1.19	11.97 ± 0.84
As	ng/m^3	23.46 ± 17.94	18.25 ± 12.34	6.77 ± 0.55	6.66 ± 0.25	8.13 ± 2.85	5.61 ± 3.79	5.99 ± 0.47	5.93 ± 0.17
Fe	ng/m^3	510.77 ± 252.72	334.38 ± 200.91	721.40 ± 167.08	577.17 ± 105.28	352.18 ± 138.62	423.81 ± 185.39	674.12 ± 124.54	621.64 ± 125.87
Cu	ng/m^3	13.12 ± 7.36	12.78 ± 5.96	8.52 ± 1.57	8.14 ± 1.22	3.15 ± 2.40	9.46 ± 8.63	73.48 ± 9.23	73.11 ± 7.52
Mn	ng/m^3	1.42 ± 0.57	4.54 ± 3.96	22.42 ± 0.04	22.40 ± 0.04	0.75 ± 0.28	2.34 ± 1.57	20.13 ± 0.03	20.12 ± 0.03
Ca	ng/m^3	392.92 ± 88.88	330.27 ± 99.02	646.91 ± 166.81	778.73 ± 68.10	633.80 ± 192.48	499.90 ± 97.10	608.19 ± 145.84	660.36 ± 54.46
Mg	ng/m^3	72.44 ± 30.34	156.53 ± 51.99	341.04 ± 66.93	398.15 ± 20.99	46.36 ± 11.93	146.33 ± 34.33	348.52 ± 100.86	334.35 ± 20.92
K	ng/m^3	349.38 ± 197.77	323.11 ± 138.27	602.98 ± 85.78	619.11 ± 65.97	494.73 ± 204.09	427.66 ± 138.97	528.32 ± 38.10	523.11 ± 31.66
Al	ng/m^3	397.36 ± 149.63	247.49 ± 77.20	634.40 ± 184.11	732.52 ± 82.65	489.11 ± 172.09	337.75 ± 117.65	533.43 ± 124.23	682.89 ± 118.93
Pb	ng/m^3	55.94 ± 35.67	59.00 ± 41.23	14.71 ± 0.10	14.92 ± 0.24	31.06 ± 14.37	30.82 ± 16.77	13.80 ± 1.43	14.36 ± 1.01
Cd	ng/m^3	20.12 ± 12.15	16.43 ± 11.11	33.86 ± 2.76	33.31 ± 1.24	2.99 ± 2.28	8.98 ± 8.19	29.97 ± 2.37	29.64 ± 0.84
Ni	ng/m^3	19.01 ± 14.54	14.79 ± 9.99	170.45 ± 31.39	162.75 ± 24.39	2.84 ± 2.17	8.53 ± 7.78	146.96 ± 18.47	146.23 ± 15.03
Cr	ng/m^3	21.12 ± 16.15	16.43 ± 11.11	135.42 ± 11.06	133.24 ± 4.94	2.81 ± 2.14	8.45 ± 7.71	119.86 ± 9.47	118.54 ± 3.36
Zn	ng/m^3	61.54 ± 39.24	64.91 ± 45.35	12.78 ± 2.35	12.21 ± 1.83	34.16 ± 15.81	33.90 ± 18.45	18.37 ± 2.31	18.28 ± 1.88
V	ng/m^3	26.38 ± 9.20	23.65 ± 6.54	354.54 ± 23.58	265.52 ± 32.1	11.24 ± 4.51	9.89 ± 4.21	125.65 ± 8.54	121.58 ± 9.45

These results strongly suggest that SO_4^{2-} coming from both northern and local anthropogenic pollution sources was still the major contributor to atmospheric PM except that its contribution during the SLBs periods was much less than the NEM periods. The mass concentration of $PM_{2.5}$ was generally higher than that of $PM_{2.5–10}$ during the PM_{10} episodes in this study. The concentration of Cl^- and Na^+ for $PM_{2.5–10}$ at offshore sites was higher than those at the inland sites. These results suggest that sea salts from oceanic spray was still the major contributor to $PM_{2.5–10}$. The replacement of chloride from sea-salt particles is caused by the accumulation of sulfate and nitrate by atmospheric particles, and nitric acid prefers to react with sodium chloride to form stable sodium nitrate (Wall *et al*., 1988, Fang *et al*., 2000).

Excess sulfate content of PM (i.e. non-sea salt sulfate, nss-$[SO_4^{2-}]$) can be estimated by subtracting the amount of SO_4^{2-} in sea salts from atmospheric SO_4^{2-}. The amount of marine sulfate was estimated from the SO_4^{2-} and Na^+ ratio of bulk seawater. The Na^+ in the atmospheric PM is assumed to originate from sea salt particles only (Colbeck and Harrison, 1984). Hence, excess SO_4^{2-} can be derived by the following equation.

$$\text{nss-}[SO_4^{2-}] = [SO_4^{2-}] - 0.231 \times [Na^+] \quad (1)$$

Table 4 shows the ionic species, carbonaceous contents and PM correlation matrix. Within the chemical composition of $PM_{2.5}$, nss-SO_4^{2-} and nitrate (NO_3^-) were strongly correlated with ammonium (NH_4^+) during the SLBs periods. The most likely chemical compounds in metro Kaohsiung would be ammonium sulfate ($(NH_4)_2SO_4$) and ammonium nitrate (NH_4NO_3). Secondary PM, mainly characterized as sulfate and nitrate, are believed to be mostly responsible for the scattering of visible light causing the degradation of visibility (Yuan *et al*., 2006). However, the ratio of chloride to sodium for $PM_{2.5x10}$ stayed almost constant for the SLBs and NEM periods. For atmospheric PM, the concentration of crustal ions (K^+ and Ca^{2+}) in the NEM periods was higher than those in the SLBs periods. However, a strong northern monsoon blew crustal ions of PM from north to south.

Carbonaceous contents of $PM_{2.5}$ and $PM_{2.5–10}$ are listed in Table 2 and the ratios of OC to EC concentrations (OC/EC) are shown in Fig. 3. The OC/EC ratios of $PM_{2.5}$ were generally higher than of $PM_{2.5–10}$ during the SLBs and NEM periods. Moreover, the OC/EC ratios at the inland sites were much higher than at the offshore sites during the SLBs and NEM periods. Carbonaceous contents of atmospheric PM at daytime during the SLBs periods higher than during the NEM periods, while an opposite trend was observed in nighttime. The OC/EC ratios of $PM_{2.5}$ ranged from 1.05 to 3.56 with an average of 2.26. It is interesting to note that the OC/EC ratio of $PM_{2.5}$ was 3.56 at inland sites during NEM periods, which is close to that in gasoline vehicle emissions (3.2) (Turpin and Huntzicker, 1995). The OC/EC ratio higher than a threshold of 2.0–2.2 indicates the potential formation of secondary aerosols (Chow *et al*., 1994; Turpin and Huntizicker, 1995). Cao *et al*. (2009) reported that annual mean concentrations of OC and EC in Hangzhou, China were 24.41 and 4.06 μg/m^3, respectively. In this study, the OC/EC ratios were lower than those measured in Xi'an (3.2) (Cao *et al*., 2005) and Hangzhou (6.0) (Cao *et al*., 2009), China, however, they were higher than those in Beijing, China (2.0) (Zhang *et al*., 2009) and in Seoul, Korea (1.3) (Park *et al*., 2002). Particularly, the average OC/EC ratios in daytime were generally higher than the threshold. The results suggest that secondary aerosols could be commonly formed during daytime in southern Taiwan. Frequent clear days and high solar intensity in southern Taiwan initiate a photochemical reaction during the NEM periods. Favorable meteorological conditions, coal combustion and VOCs emitted from industrial, power plants and mobile sources both in the northern and local regions resulted in higher OC/EC ratios during the NEM periods and were higher than those during the SLBs periods (Cao *et al*., 2003). Moreover, a strong northerly wind blew a huge amount of VOCs from the north to the south.

Fig. 4 illustrates the metallic contents of $PM_{2.5}$ and $PM_{2.5–10}$ at inland and offshore sites in southern Taiwan. The correlation matrix of metallic contents and atmospheric PM is shown in Table 5. The most abundant metallic elements in the atmospheric $PM_{2.5–10}$ were crustal elements, including Ca, Fe, and Al (Fig. 4) during the SLBs and NEM periods. Other metals, such as Mg, Pb, V, and Zn were also enriched in the atmospheric PM. Regardless of the periods (SLBs or NEM), a high concentration of Mg was consistent with ionic species (Mg^{2+}) of $PM_{2.5}$ and $PM_{2.5–10}$ at offshore sites. The most abundant metallic elements were Ca and Fe for both fine and coarse particles, respectively. An increase of Ni and V concentration is typically observed in the fuel burning sources (Hung *et al*., 1994; Lee *et al*., 1994) is due to the relative weight of this source emission during the NEM periods. The concentration of Zn and Pb in the SLBs periods was always higher than those in the NEM periods. This is true for Zn, Pb, and Fe typically associated with traffic emission (Weckwerth, 2001; Sternbeck *et al*., 2002; Chellam *et al*., 2005). Although the distribution of metallic elements was similar to some extent, the differences between the SLBs and NEM periods were identified. The order of major metallic elements of atmospheric $PM_{2.5}$ during the SLBs and NEM periods is Fe > Ca > K > Al > Mg > Zn > Pb and Ca > Fe > Al > K > Mg > V > Ni, respectively. The composition of the atmospheric $PM_{2.5–10}$ during the SLBs and NEM periods is Ca > K > Al > Fe > Mg > Zn and Fe > Ca > Al > K > Mg > V > Ni, respectively.

The analysis of enrichment factors (EF) relative to earth's crust composition can be used to identify the origins of elements from crustal or anthropogenic sources (Taylor &McLennan, 1995). The chemical species of field measured particulates were compared with a reference element (Al) as shown in below,

$$EF_{crust} = \frac{(C_{element}/C_{refercence})_{air}}{(C_{element}/C_{reference})_{crust}} \quad (2)$$

Table 4. Correlation matrix of ionic species, carbonaceous contents, $PM_{2.5}$ and $PM_{2.5–10}$ in the coastal region of southern Taiwan.

SLBs-$PM_{2.5}$	F^-	Cl^-	NO_3^-	nss-SO_4^{2-}	Na^+	NH_4^+	K^+	Mg^{2+}	Ca^{2+}	EC	TC	OC	$PM_{2.5}$
F^-	1.00												
Cl^-	0.37	1.00											
NO_3^-	0.20	0.19	1.00										
nss-SO_4^{2-}	0.00	0.09	0.69	1.00									
Na^+	0.35	0.90	0.41	0.56	1.00								
NH_4^+	0.43	0.31	0.72	0.75	0.22	1.00							
K^+	0.56	0.52	0.40	0.06	0.47	0.60	1.00						
Mg^{2+}	0.15	0.62	0.02	0.14	0.66	0.23	0.37	1.00					
Ca^{2+}	0.26	0.35	0.31	0.34	0.28	0.40	0.25	0.55	1.00				
EC	–0.24	0.47	0.55	0.55	0.43	0.40	0.18	0.40	0.29	1.00			
TC	–0.08	0.22	0.71	0.66	0.15	0.50	0.18	0.22	0.32	0.83	1.00		
OC	0.00	0.09	0.70	0.65	0.02	0.49	0.17	0.12	0.30	0.67	0.97	1.00	
$PM_{2.5}$	–0.02	0.14	0.83	0.81	0.07	0.72	0.16	0.01	0.26	0.61	0.72	0.69	1.00
NEM-$PM_{2.5}$	F^-	Cl^-	NO_3^-	nss-SO_4^{2-}	Na^+	NH_4^+	K^+	Mg^{2+}	Ca^{2+}	EC	TC	OC	$PM_{2.5}$
F^-	1.00												
Cl^-	–0.35	1.00											
NO_3^-	–0.24	0.77	1.00										
nss-SO_4^{2-}	0.41	–0.13	0.56	1.00									
Na^+	–0.33	0.85	0.27	0.10	1.00								
NH_4^+	0.49	–0.23	0.03	0.94	–0.21	1.00							
K^+	–0.50	0.47	0.76	0.28	0.48	0.08	1.00						
Mg^{2+}	–0.32	0.15	0.30	0.46	0.17	0.20	0.57	1.00					
Ca^{2+}	–0.30	0.71	0.58	0.09	0.70	–0.06	0.70	0.40	1.00				
EC	0.28	–0.02	–0.01	0.41	0.01	0.37	–0.04	0.01	–0.02	1.00			
TC	0.01	0.37	0.32	0.16	0.38	0.11	0.12	0.01	0.22	0.81	1.00		
OC	0.23	0.08	0.07	0.36	0.10	0.32	0.00	0.01	0.04	0.99	0.89	1.00	
$PM_{2.5}$	–0.06	0.32	0.72	0.85	0.36	0.65	0.40	0.20	0.35	0.72	0.69	0.74	1.00
SLBs-$PM_{2.5–10}$	F^-	Cl^-	NO_3^-	nss-SO_4^{2-}	Na^+	NH_4^+	K^+	Mg^{2+}	Ca^{2+}	EC	TC	OC	$PM_{2.5–10}$
F^-	1.00												
Cl^-	–0.17	1.00											
NO_3^-	0.04	0.08	1.00										
nss-SO_4^{2-}	0.24	–0.13	0.72	1.00									
Na^+	–0.23	0.99	0.66	0.45	1.00								
NH_4^+	0.22	–0.06	0.67	0.61	–0.07	1.00							
K^+	0.31	0.32	0.49	0.26	0.29	0.58	1.00						
Mg^{2+}	0.13	0.60	0.21	0.36	0.76	0.09	0.33	1.00					
Ca^{2+}	0.41	0.08	0.51	0.60	0.06	0.43	0.45	0.65	1.00				
EC	–0.14	0.52	0.53	0.46	0.52	0.52	0.42	0.58	0.46	1.00			
TC	–0.10	0.32	0.73	0.63	0.31	0.57	0.44	0.51	0.54	0.89	1.00		
OC	–0.07	0.20	0.77	0.66	0.18	0.55	0.42	0.43	0.54	0.77	0.98	1.00	
$PM_{2.5–10}$	–0.09	0.70	0.75	0.46	0.78	0.51	0.57	0.41	0.56	0.73	0.81	0.79	1.00
NEM-$PM_{2.5–10}$	F^-	Cl^-	NO_3^-	nss-SO_4^{2-}	Na^+	NH_4^+	K^+	Mg^{2+}	Ca^{2+}	EC	TC	OC	$PM_{2.5–10}$
F^-	1.00												
Cl^-	0.12	1.00											
NO_3^-	0.32	0.20	1.00										
nss-SO_4^{2-}	0.79	–0.32	0.31	1.00									
Na^+	0.14	0.96	0.22	0.30	1.00								
NH_4^+	0.90	–0.11	0.31	0.81	–0.11	1.00							
K^+	0.07	0.11	0.62	0.10	0.14	–0.24	1.00						
Mg^{2+}	0.34	–0.12	0.16	0.57	–0.11	0.17	0.36	1.00					
Ca^{2+}	0.41	0.03	0.61	0.22	0.05	–0.05	0.90	0.40	1.00				
EC	0.43	0.39	0.58	0.35	0.40	0.33	0.37	0.23	0.28	1.00			
TC	–0.02	0.75	0.30	–0.15	0.75	–0.03	0.19	0.00	0.03	0.66	1.00		
OC	0.29	0.55	0.53	0.20	0.56	0.23	0.34	0.17	0.22	0.96	0.84	1.00	
$PM_{2.5–10}$	0.16	0.61	0.46	0.42	0.62	0.16	0.31	0.11	0.62	0.82	0.80	0.88	1.00

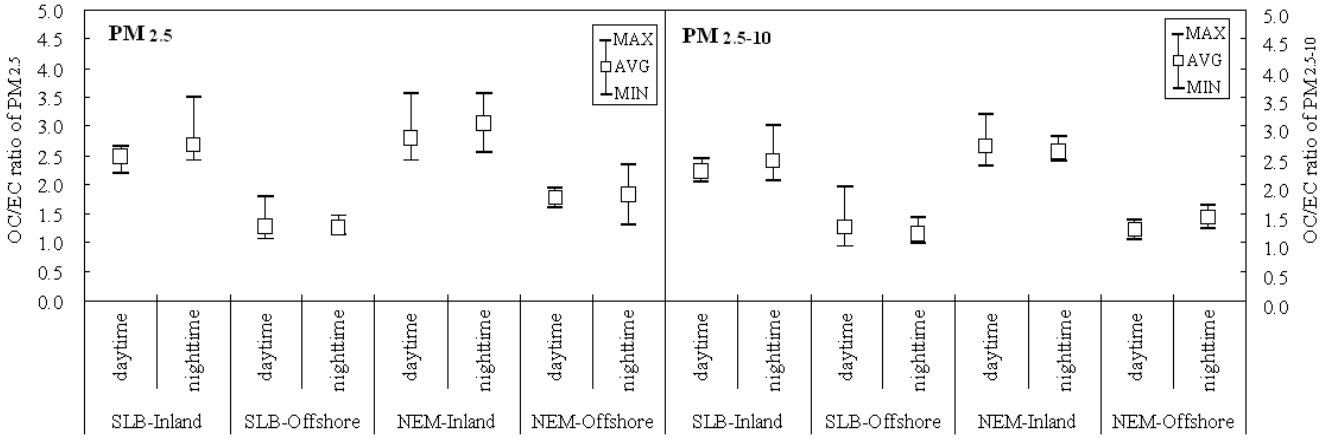

Fig. 3. OC/EC ratio of $PM_{2.5}$ and $PM_{2.5–10}$ during daytime and nighttime at the sampling sites in the SLBs and NEM periods.

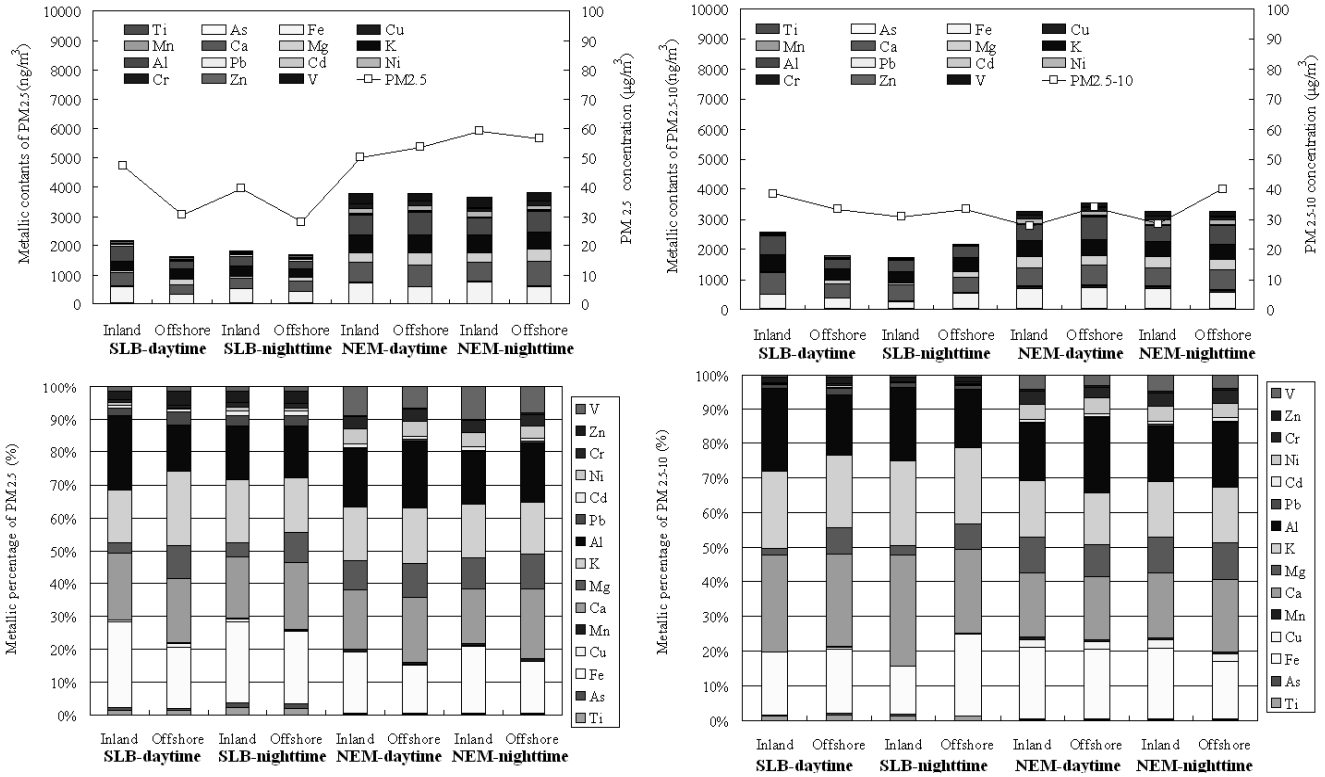

Fig. 4. Metallic content and percentage of $PM_{2.5}$ and $PM_{2.5–10}$ during daytime and nighttime at the sampling sites in the SLBs and NEM periods.

where $C_{element}$ is the concentration of any elements, and $C_{refercence}$ is the concentration of the reference element. Typically, Al, Si, Fe was chosen as the reference element, of which Al was used in this study. As shown Fig. 5, comparative analysis of EF values was however limited on PM data sets; this is because all the computation is conducted to compare the concentration ratios in all airborne particles against those ratios representing earth's crust. If the computed EF values for a given element exceeds far above unity (e.g., EF > 10), it can imply that the extent of enrichment is significant for that element compared to its crustal composition (Cao *et al*., 2009; Alleman *et al*., 2010). It was seen that several toxic metals like Pb, Ni, As, Zn, Cu, Ti, V, and Cd showed EF values above a few tens or hundreds, suggesting the possibly important role of anthropogenic sources. However in accord with the general expectation, most of crustal components showed much smaller values of < 10(Ca, Fe, Mn, Mg, Cr and K). In addition, K element was influenced not only by crustal (soil dust) but also by anthropogenic sources (biomass burning) (Cao *et al*., 2009). Similarly to our researches, Cao *et al*. (2009) also observed consistently low EF values for crustal components by conducting field measurements of PM_{10} from five distinctive urban locations

Table 5. Correlation matrix of metallic contents, $PM_{2.5}$ and $PM_{2.5–10}$ in the coastal region of southern Taiwan.

SLBs-$PM_{2.5}$	Ti	As	Fe	Cu	Mn	Ca	Mg	K	Al	Pb	Cd	Ni	Cr	Zn	V	$PM_{2.5}$
Ti	1.00															
As	0.32	1.00														
Fe	0.23	0.12	1.00													
Cu	0.25	0.23	0.51	1.00												
Mn	0.09	0.09	–0.03	0.10	1.00											
Ca	–0.07	–0.07	0.66	0.31	–0.35	1.00										
Mg	–0.19	–0.19	–0.42	–0.03	0.23	–0.52	1.00									
K	0.07	0.07	0.72	0.52	0.13	0.39	–0.11	1.00								
Al	0.18	0.18	0.69	0.18	0.07	0.38	–0.39	0.33	1.00							
Pb	0.29	0.29	0.59	0.44	0.08	0.20	0.07	0.51	0.38	1.00						
Cd	0.27	1.00	0.43	0.23	0.05	–0.07	–0.19	0.07	0.12	0.21	1.00					
Ni	0.11	0.12	0.23	0.25	0.10	0.05	0.17	0.11	0.15	0.19	1.00	1.00				
Cr	0.16	0.35	0.24	0.13	0.12	0.13	–0.09	0.12	0.18	0.08	0.23	0.24	1.00			
Zn	0.29	0.29	0.59	0.44	0.08	0.20	0.07	0.51	0.38	0.10	0.29	0.25	0.21	1.00		
V	0.13	0.23	0.60	0.36	0.32	0.17	0.21	0.36	0.45	0.21	0.16	0.54	0.05	0.14	1.00	
$PM_{2.5}$	0.33	0.33	0.52	0.20	-0.02	0.51	0.67	0.62	0.48	0.40	0.33	0.33	0.33	0.47	0.55	1.00
NEM-$PM_{2.5}$	Ti	As	Fe	Cu	Mn	Ca	Mg	K	Al	Pb	Cd	Ni	Cr	Zn	V	$PM_{2.5}$
Ti	1.00															
As	0.09	1.00														
Fe	–0.06	–0.03	1.00													
Cu	–0.19	0.09	0.50	1.00												
Mn	–0.17	0.29	0.59	0.81	1.00											
Ca	0.40	0.08	0.15	0.32	0.26	1.00										
Mg	0.34	0.02	0.07	0.37	0.28	0.93	1.00									
K	0.05	0.18	0.20	0.79	0.76	0.53	0.58	1.00								
Al	0.21	0.31	0.60	–0.24	–0.02	–0.10	–0.24	–0.15	1.00							
Pb	0.32	0.10	–0.06	–0.19	–0.17	0.39	0.34	0.00	0.21	1.00						
Cd	0.09	0.12	–0.03	0.09	0.30	0.08	0.02	0.18	0.31	0.10	1.00					
Ni	0.15	0.09	0.50	0.13	0.81	0.32	0.37	0.39	0.33	–0.19	0.09	1.00				
Cr	0.11	0.21	0.03	0.08	0.30	0.08	0.02	0.18	0.31	0.10	0.20	0.09	1.00			
Zn	–0.19	0.09	0.50	0.02	0.82	0.32	0.37	0.79	–0.24	–0.19	0.19	0.05	0.09	1.00		
V	0.21	0.13	0.71	0.21	0.44	0.38	0.27	0.12	0.66	0.32	0.10	0.79	0.08	0.41	1.00	
$PM_{2.5}$	–0.28	–0.34	0.46	0.30	0.09	0.56	0.24	0.22	0.51	–0.28	–0.34	0.30	–0.34	0.40	0.62	1.00
SLBs-$PM_{2.5–10}$	Ti	As	Fe	Cu	Mn	Ca	Mg	K	Al	Pb	Cd	Ni	Cr	Zn	V	$PM_{2.5–10}$
Ti	1.00															
As	0.14	1.00														
Fe	0.55	–0.39	1.00													
Cu	0.37	0.03	0.21	1.00												
Mn	0.52	–0.04	0.59	0.45	1.00											
Ca	0.36	–0.05	0.48	0.02	–0.02	1.00										
Mg	–0.01	–0.28	0.26	0.10	0.42	–0.30	1.00									
K	0.37	–0.17	0.35	–0.18	–0.10	0.57	0.64	1.00								
Al	0.43	–0.01	0.38	0.15	–0.04	0.67	–0.38	0.73	1.00							
Pb	0.21	0.15	0.65	0.37	0.55	0.36	–0.01	0.37	0.43	1.00						
Cd	0.30	0.03	0.21	0.12	0.45	0.18	0.12	0.12	0.18	0.31	1.00					
Ni	0.37	0.13	0.20	0.25	0.21	0.01	0.16	–0.18	0.15	0.27	0.30	1.00				
Cr	0.12	0.22	0.11	0.32	0.35	0.37	0.10	0.12	0.28	0.37	0.13	0.23	1.00			
Zn	0.20	0.14	0.35	0.37	0.52	0.36	–0.01	0.37	0.43	0.20	0.37	0.24	0.35	1.00		
V	0.32	0.11	0.32	0.35	0.37	0.27	0.52	0.18	0.52	0.33	0.11	0.52	0.32	0.32	1.00	
$PM_{2.5–10}$	0.48	–0.06	0.67	0.17	0.34	0.64	0.50	0.50	0.63	0.48	0.17	0.17	0.17	0.48	0.45	1.00
NEM-$PM_{2.5–10}$	Ti	As	Fe	Cu	Mn	Ca	Mg	K	Al	Pb	Cd	Ni	Cr	Zn	V	$PM_{2.5–10}$
Ti	1.00															
As	0.45	1.00														
Fe	0.31	0.20	1.00													
Cu	0.16	–0.22	0.23	1.00												
Mn	0.22	–0.15	0.65	0.38	1.00											

Table 5. *(continued).*

NEM-$PM_{2.5–10}$	Ti	As	Fe	Cu	Mn	Ca	Mg	K	Al	Pb	Cd	Ni	Cr	Zn	V	$PM_{2.5–10}$
Ca	0.46	0.28	0.28	0.34	0.29	1.00										
Mg	0.15	0.03	0.16	0.19	0.17	0.73	1.00									
K	0.09	–0.18	0.47	0.61	0.64	0.57	0.39	1.00								
Al	0.18	0.24	0.33	–0.19	0.22	0.16	0.36	0.40	1.00							
Pb	0.20	0.45	0.31	0.16	0.22	0.46	0.15	0.09	0.18	1.00						
Cd	0.45	0.18	0.23	–0.22	–0.15	0.28	0.02	–0.18	0.14	0.25	1.00					
Ni	0.16	0.32	0.23	0.47	0.43	0.24	0.32	0.58	0.15	0.16	0.21	0.12				
Cr	0.32	0.23	0.20	0.13	0.18	0.25	0.03	0.15	0.27	0.45	0.28	–0.22	1.00			
Zn	0.16	–0.12	0.23	0.20	0.33	0.32	0.19	0.61	–0.19	0.16	0.02	0.10	0.18	1.00		
V	0.21	0.10	0.54	0.32	0.30	0.22	0.12	0.27	0.41	0.32	0.07	0.68	0.09	0.17	1.00	
$PM_{2.5–10}$	0.33	–0.17	0.69	0.44	0.12	0.66	0.14	0.46	0.65	0.33	–0.17	0.44	–0.17	0.44	0.54	1.00

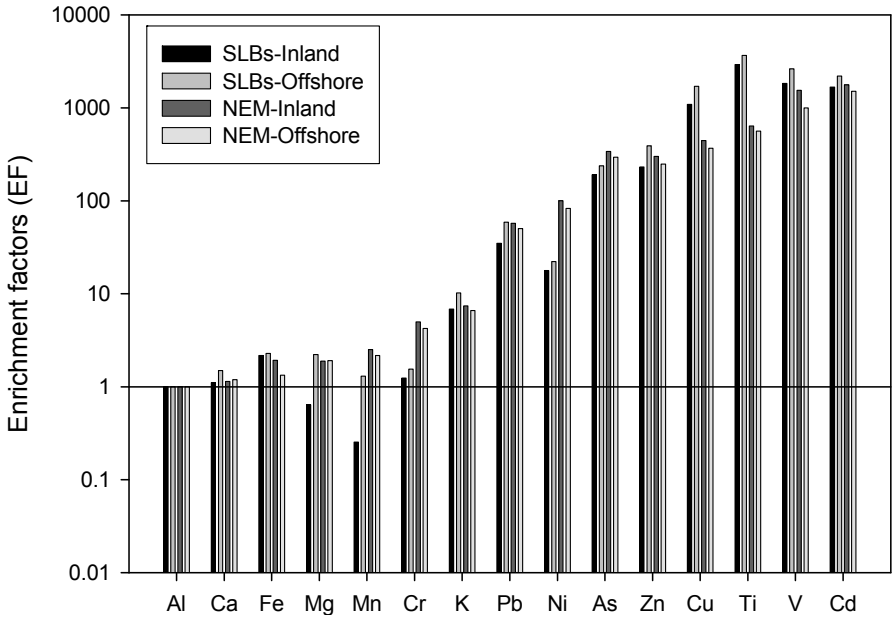

Fig. 5. Enrichment factors (EF) of PM at during the SLBs and NEM periods.

in Hangzhou, China. The previous studies made in sampling sites around the other countries are also highly compatible with the results of this study (Alleman *et al*., 2010).

Effects of Sea-land Breeze and Northeastern Monsoon

A backward trajectory model is used to determine the transportation routes of PM before they arrived at the sampling locations. Backward trajectory modeling involves tracing the transportation of air parcel through the meteorological wind field. Prior to modeling, the meteorological data (wind velocity and direction) of the transportation of air mass were gathered from the Taiwan Environmental Protection Administration and Taiwan Central Weather Bureau. In addition, a three-dimension wind field, including wind speed and direction, was used to determine the transportation routes of suspended particles in the backward trajectory model. The backward trajectories of the air parcel transported toward the inland air quality monitoring sites around the coastal region of southern Taiwan during the SLBs and NEM periods are illustrated in Fig. 6. It showed that, during the SLBs periods, sea breezes blown in the early morning could transport the offshore PM back inland in southern Taiwan, which resulted in relatively high PM concentration at inland sites in the afternoon. On the contrary, high PM concentrations observed during the NEM periods were mainly blown by NEM which transported the cross-boundary PM from north to south. Backward trajectories also indicated that sea breezes could further blow offshore cross-boundary PM east of metro Kaohsiung.

A previous study revealed that HNO_3 prefers to react with NaCl to form stable $NaNO_3$ in the coarse mode (Wall *et al*., 1988). The regression between Na^+ with nss-$[SO_4^{2-}]$ and NO_3^- concentrations obtained in the present study is shown in Fig. 6. The separate nss-$[SO_4^{2-}]/[Na^+]$ and $[NO_3^-]/[Na^+]$ lines represent two different sources in the offshore and inland regions. During the SLBs periods, the nss-$[SO_4^{2-}]$ to $[Na^+]$ slope of $PM_{2.5–10}$ at the offshore and inland sites were 0.837 and 0.625, respectively, as illustrated in Fig. 7(a). The nss-$[SO_4^{2-}]/[Na^+]$ and $[NO_3^-]/[Na^+]$ of $PM_{2.5–10}$ was more stable than $PM_{2.5}$ during the SLBs periods. Compared to $[Na^+]$ and nss-$[SO_4^{2-}]$, $[Na^+]$ and $[NO_3^-]$ as a

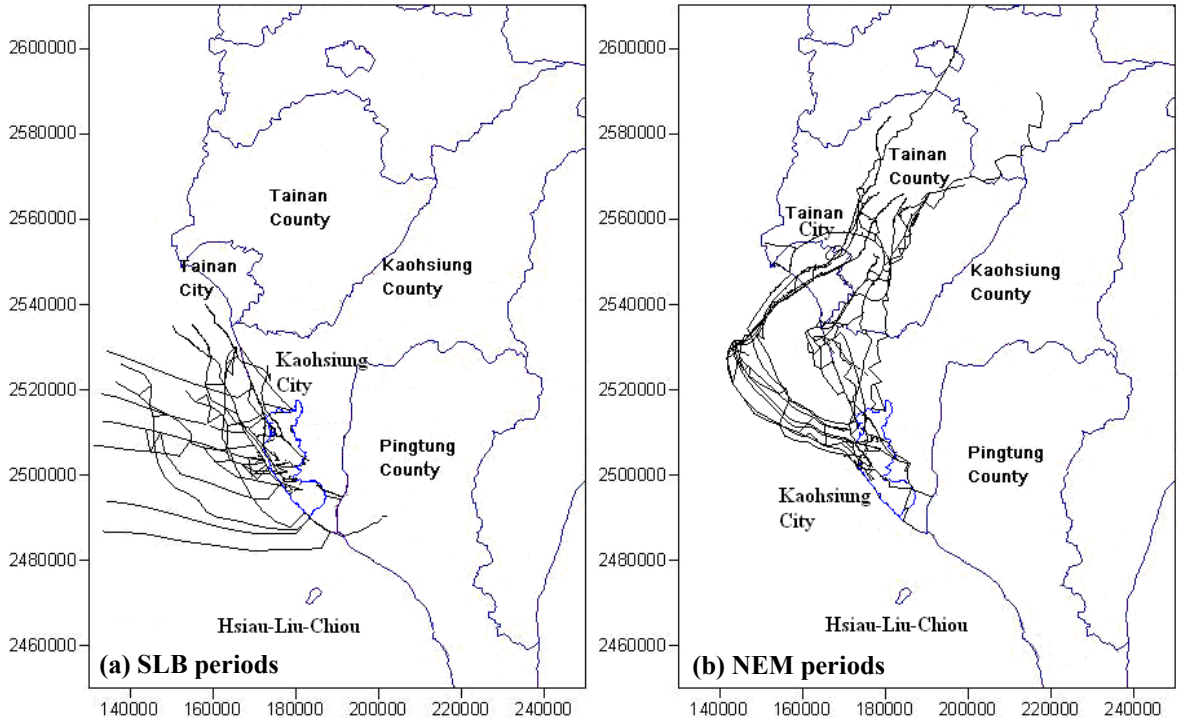

Fig. 6. Backward trajectories of air parcel transported toward the inland sites in the coastal region of southern Taiwan during (a) SLBs and (b) NEM periods (x- and y-axis legends are UTM in meter).

PM pollutant index can differentiate PM collected at offshore and inland sites. The regression slope of $[NO_3^-]$ to $[Na^+]$ for $PM_{2.5}$ and $PM_{2.5–10}$ at inland sites is higher than at the offshore sites during the SLBs periods. Moreover, the regression slopes are different between the inland and offshore sites, indicating that atmospheric PM was not emitted from the same sources. Fig. 7(c) and 7(d) illustrate the slopes of nss-$[SO_4^{2-}]/[Na^+]$ and $[NO_3^-]/[Na^+]$ for $PM_{2.5}$ and $PM_{2.5–10}$ during the NEM periods. The regression slopes of nss-$[SO_4^{2-}]/[Na^+]$ for $PM_{2.5}$ at the inland sites were 11.51 and 1.730, respectively, and the point of $[NO_3^-]/[Na^+]$ separate more diversely than nss-$[SO_4^{2-}]/[Na^+]$ as shown in Fig. 7(d). Although similar trends were observed during the NEM periods, the nss-$[SO_4^{2-}]/[Na^+]$ ratio regarding the PM pollutant index was more suitable than the $[NO_3^-]/[Na^+]$ ratio. Fig. 7 illustrates that the slopes of nss-$[SO_4^{2-}]/[Na^+]$ and $[NO_3^-]/[Na^+]$, could due to anthropogenic and natural pollution sources during the SLBs and NEM periods.

CONCLUSIONS

The effects of SLBs and the northeastern monsoon on the physicochemical properties of atmospheric aerosols over southeastern coastal region of Taiwan Strait were investigated in this study. Strong SLBs were regularly observed during the monitoring periods (I), (II), and (V). However, no significant SLBs appeared in the coastal region of southern Taiwan during the sampling periods (III) and (IV). Meteorological and model simulation results showed that PM could be transported back and forth across the coastline in the investigation region. The $PM_{2.5}/PM_{10}$ ratios during the NEM periods were always higher than those during the SLBs periods. The most abundant ionic species of PM were: SO_4^{2-}, NO_3^- and NH_4^+. The most likely chemical compounds at Kaohsiung region would be $((NH_4)_2SO_4)$ and (NH_4NO_3). The carbon content of atmospheric aerosol particles during the NEM periods was higher than during the SLBs periods. The OC/EC ratio of $PM_{2.5}$ ranged from 1.05 to 4.39 with an average of 2.26. The order of major metallic elements of atmospheric $PM_{2.5}$ for the SLBs and NEM periods is Fe > Ca > K > Al > Mg > Zn > Pb and Ca > Fe > Al > K > Mg > V > Ni, respectively, and atmospheric $PM_{2.5–10}$ is Ca > K > Al > Fe > Mg > Zn and Fe > Ca > Al > K > Mg > V > Ni, respectively. The results of the nss-$[SO_4^{2-}]/[Na^+]$ ratio was more suitable for a PM pollution index than was the $[NO_3^-]/[Na^+]$ ratio. This study revealed that the accumulation of particulate matter in the near-ocean region due to sea-land breeze had a regular influence on the physicochemical properties of PM in the coastal region of southern Taiwan. The results indicated that the atmospheric PM might not be emitted from the same source during the sampling periods.

ACKNOWLEDGMENTS

This study was performed under the auspices of Environmental Protection Bureau of Kaohsiung Municipal Government. The authors are grateful to the CENPRO Technology Limited Company, the KELEE Environmental Consultant Corporation, the ENVIMAC Technology and Consultant Corporation, and the SOUTHERN TAIWAN Environmental Consultant Corporation for their assistance in sampling PM for this study.

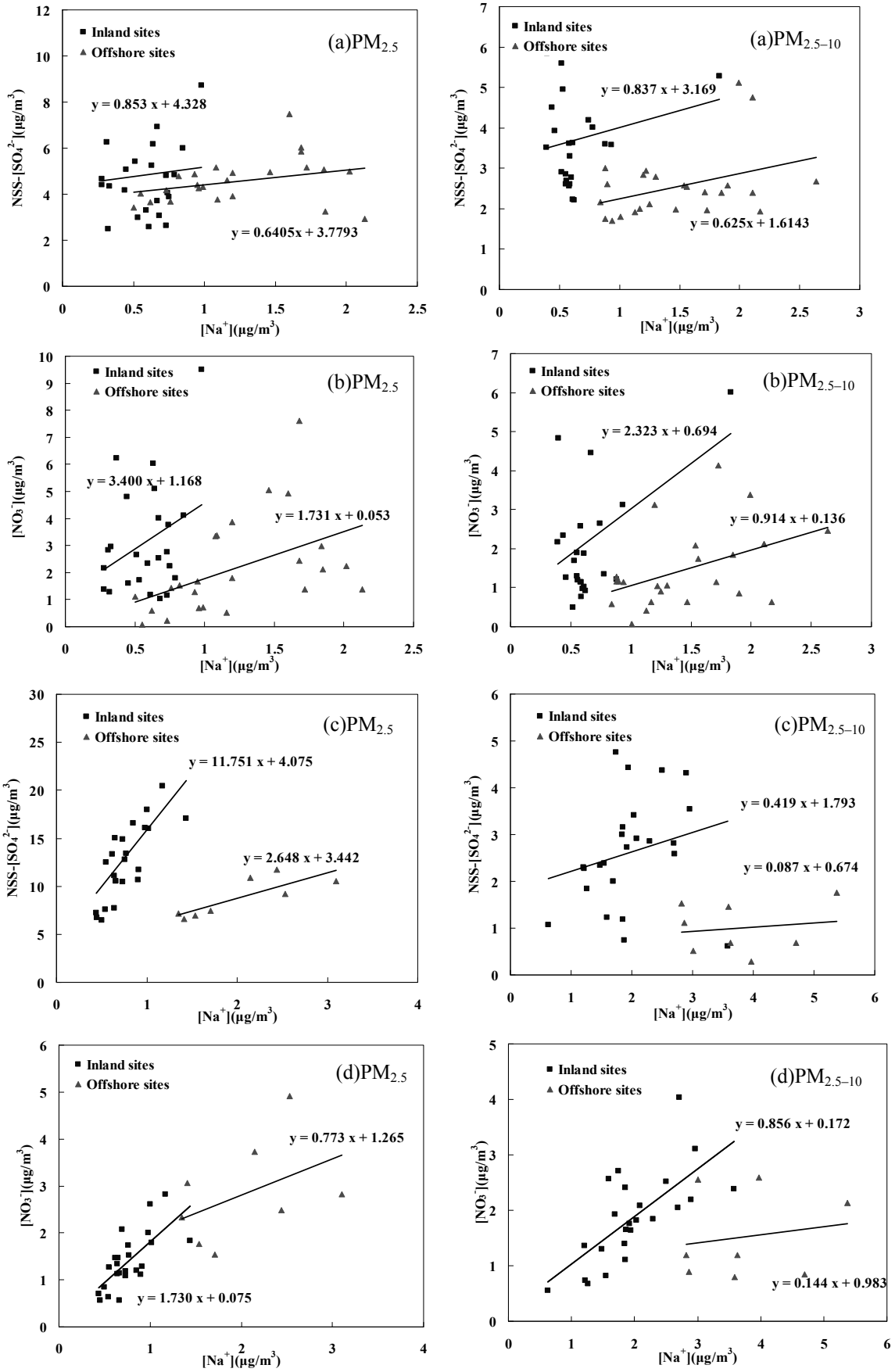

Fig. 7. nss-[SO_4^{2-}] to [Na^+] and [NO_3^-] to [Na^+] ratios for $PM_{2.5}$ and $PM_{2.5–10}$ during (a) (b) SLBs and (c) (d) NEM periods.

REFERENCES

Alleman, L.Y., Lamaison, L., Perdrix, E., Robache, A. and Galloo, J.C. (2010). PM_{10} Metal Concentrations and Source Identification Using Positive Matrix Factorization and Wind Sectoring in a French Industrial Zone. *Atmos. Res.* 96: 612–625.

Brook, J.R., Wiebe, A.H., Woodhouse, S.A., Audette, C.V., Dann, T.F., Dann, T.F., Callaghan, S., Piechowski, M., Dabek-Zlotorzynska, E. and Dloughy, J.F. (1997). Temporal and Spatial Relationships in Fine Particle Strong Acidity, Sulphate, PM_{10}, and $PM_{2.5}$ Across Multiple Canadian locations. *Atmos. Environ.* 31: 4223–4236.

Byun, D.W., Kim, S.T. and Kim, S.B. (2007). Evaluation of Air Quality Models for the Simulation of a High Ozone Episode in the Houston Metropolitan Area. *Atmos. Environ.* 41: 837–853.

Cao, J.J., Lee, S.C., Ho, K.F., Zou, S.C., Zhang, X.Y. and Pan, J.G. (2003). Spatial and Seasonal Distributions of Atmospheric Carbonaceous Aerosols in Pearl River Delta Region, China. *China Particuology* 1: 33–37.

Cao, J.J., Wu, F., Chow, J.C., Lee, S.C., Li, Y., Chen, S.W., An, Z.S., Fung, K., Watson, J.G., Zhu, C.S. and Liu, S.X. (2005). Characterization Source Apportionment of Atmospheric Organic and Elemental Carbon during Fall and Winter of 2003 in Xi'an, China. *Atmos. Chem. Phys.* 5: 3127–3137.

Cao, J.J., Shen Z.X., Chow .J.C., Qi, G.W. and Watson, J.G. (2009). Seasonal Variations and Sources of Mass and Chemical Composition for PM_{10} Aerosol in Hangzhou, China. *Particuology* 7: 161–168.

Chellam, S., Kulkarni, P. and Fraser, M.P. (2005). Emissions of Organic Compound and Trace Metals in Fine Particulate Matter from Motor Vehicles: A Tunnel Study in Houston, Texas. *J. Air Waste Manage. Assoc.* 55: 60–72.

Cheng, W.L. (2002). Ozone Distribution in Coastal Central Taiwan under Sea-breeze Conditions. *Atmos. Environ.* 36: 3445–3459.

Chow, J.C., Watson J.G., Fujita, E.M., Lu, Z. and Lawson, D.R. (1994). Temporal and Spatial Variation of $PM_{2.5}$ and PM_{10} Aerosol in Southern California Air Quality Study. *Atmos. Environ.* 28: 2061–2080.

Colbeck, I. and Harrison, R.M. (1984). Ozone-secondary Aerosol-visibility Relationships in North-west England. *Sci. Total Environ.* 34: 87–100.

Ding, A., Wang, Tao, Zhao, Ming, Wang, T. and Li, Z. (2004). Simulation of Sea-land Breezes and a Discussion of their Implications on the Transport of Air Pollution during a Multi-day Ozone Episode in the Pearl River Delta of China. *Atmos. Environ.* 38: 6737–6750.

Evtyugina, M.G., Nunes, T., Pio, C. and Costa, C.S. (2006). Photochemical Pollution under Sea Breeze Conditions, during Summer, at the Portuguese West Coast. *Atmos. Environ.* 40: 6277–6293.

Fang, G.C., Chang, C.N., Wu, Y.S., Wang, N.P. Wang, V., Fu, P.P.C., Yang, D.G. and Chen, S.C. (2000). Comparison of Particulate Mass, Chemical Species for Urban, Suburban and Rural Areas in Central Taiwan, Taichung. *Chemosphere* 41: 1349–1359.

Hien, P.D., Bac, V.T., Tham, H.C., Nhan, D.D. and Vinh, L.D. (2002). Influence of Meteorological Conditions on $PM_{2.5}$ and $PM_{2.5-10}$ Concentrations during the Monsoon season in Hanoi, Vietnam. *Atmos. Environ.* 36: 3473–3484.

Huang, X., Olmez, I. and Aras, N.K. (1994). Emissions of Trace Elements from Motor Vehicles: Potential Marker Elements and Source Composition Profile. *Atmos. Environ.* 28: 1385–1391.

Hueglin, C., Gehrig, R., Baltensperger, U., Gysel, M., Monn, C. and Vonmont, H. (2005). Chemical Characterisation of $PM_{2.5}$, PM_{10} and Coarse Particle at Urban, Near-city and Rural Sites in Switzerland. *Atmos. Environ.* 39: 637–651.

Kambezidis, H.D., Weidauer, D., Melas, D. and Ulbricht, M. (1998). Air Quality in the Athens Basin during Sea Breeze and Non-sea Breeze Day Using Laser-remote-sensing Technique. *Atmos. Environ.* 32: 2173–2182.

Lee, D.S., Garland, A. and Fox, A.A. (1994). Atmospheric Concentrations of Trace Elements in Urban Areas of the United Kingdom. *Atmos. Environ.* 28: 2691–2713.

Lee, H.S. and Kang, B.W. (2001). Chemical Characteristics of Principal $PM_{2.5}$ Species in Chongju, Southern Korea. *Atmos. Environ.* 35: 739–746.

Levin, Z., Gershon, H. and Ganor E. (2005). Vertical Distribution of Physical and Chemical Properties of Haze Particles in the Dead Sea Valley. *Atmos. Environ.* 39: 4937–4945.

Lin, J.J. (2002). Characterization of the Major Chemical Species in $PM_{2.5}$ in the Kaohsiung City, Taiwan. *Atmos. Environ.* 36: 1911–1920.

Lin, C.Y., Wang, Z., Chou, C.C.K., Chang, C.C. and Liu, S.C. (2007). A Numerical Study of an Autumn High Ozone Episode over Southwestern Taiwan. *Atmos. Environ.* 41: 3684–3701.

Liu, K.Y., Wang, Z. and Hsiao, L.F. (2002). A Modeling of the Sea Breeze and its Impacts on Ozone Distribution in Northern Taiwan. *Environ. Modell. Softw.* 17: 21–27.

Nester, K. (1995). Influence of Sea Breeze Flows on Air Pollution over the Attica Peninsula. *Atmos. Environ.* 29: 3655–3670.

Oanh, N.T.K., Upadhyay, N., Zhuang, Y.H., Hao, Z.P., Murthy, D.V.S., Lestari, P., Villarin, J.T., Chengchua, K., Co, H.X., Dung, N.T. and Lindgren E.S. (2006) Particulate Air Pollution in Six Asian Cities: Spatial and Temporal Distributions, and Associated Sources. *Atmos. Environ.* 40: 3367–3370.

O'Dowd, C.D., Smith, M.H., Consterdine, I.E. and Lowe, J.A. (1997). Marine Aerosol, Sea-salt and the Marine Sulphur Cycle: A Short Review. *Atmos. Environ.* 31: 73–80.

Pandis, S.N., Harley, R.A., Cass, G.R. and Seinfeld J.H. (1992). Secondary Organic Aerosol Formation and Transport. *Atmos. Environ.* 26: 2269–2282.

Park, S.S., Kim, Y.J. and Fung, K. (2002). $PM_{2.5}$ Carbon Measurements in Two Urban Areas: Seoul and Kwangju, Korea. *Atmos. Environ.* 36: 1287–1297.

Pankow, J.F. (1994). An Adsorption Model of the

Gas/Aerosol Partitioning Involved in the Formation of Secondary Organic Aerosol. *Atmos. Environ.* 28: 189–193.

Rodríguez, S., Querol, X., Alastuey, A. and Mantilla, E. (2002). Origin of High Summer PM_{10} and TSP Concentrations at Rural Sites in Eastern Spain. *Atmos. Environ.* 36: 3101–3112.

Smith, S., Stribley, F.T., Milligan, P. and Barratt, B. (2001). Factors Influencing Measurements of PM_{10} during 1995-1997 in London. *Atmos. Environ.* 35: 4651–4662.

Sternbeck, J., Sjödin, Å. and Andréasson, K. (2002). Metal Emission from Road Traffic and the Influence of Resuspension-results from Two Tunnel Studies. *Atmos. Environ.* 36: 4735–4744.

Taylor, S.R. and McLennan, S.M. (1995). The Geochemical Evolution of the Continental Crust. *Rev. Geophys.* 33: 241–265.

Tsai, H.H., Ti, T.H. Yuan, C.S., Hung, C.H. and Lin, C. (2008). Effects of Sea-land Breezes on the Spatial and Temporal Distribution of Gaseous Air Pollutants around the Coastal Region of Southern Taiwan. *J. Environ. Eng. Manage.* 18: 387–396.

Tsai, H.H., Yuan, C.S., Hung, C.H. and Lin, Y.C. (2010). Comparing Physicochemical Properties of Ambient Particulate Matter of Hot Spots in a Highly Polluted Air Quality Zone. *Aerosol Air Qual. Res.* 10: 331–344.

Tsai, Y.I. and Chen, C.L. (2006). Atmospheric Aerosol Composition and Source Apportionments to Aerosols in Southern Taiwan. *Atmos. Environ.* 40: 4751–4763.

Turpin, B.J. and Huntzicker, J.J. (1995). Identification of Secondary Organic Aerosol Episodes and Quantification of Primary and Secondary Organic Aerosol Concentrations during SCAQR. *Atmos. Environ.* 29: 3527–3544.

Turnbull, A.B. and Harrison, R.M. (2000). Major Component Contribution to PM_{10} Composition in the UK Atmosphere. *Atmos. Environ.* 34: 3129–3137.

Wall, S.M., John. W. and Ondo, J.L. (1988). Measurement of Aerosol Size Distributions for Nitrate and Ionic Species. *Atmos. Environ.* 22: 1649–1656.

Weckwerth, G. (2001). Verification of Traffic Emitted Aerosol Components in the Ambient Air of Cologne (Germany). *Atmos. Environ.* 35: 5525–5536.

Wyers, G.P. and Duyzer, J.H. (1997). Micrometeorological Measurement of the Dry Deposition Flux of Sulphate and Nitrate Aerosols to Coniferous Forest. *Atmos. Environ.* 31: 333–343.

Venkatesan, R., Mathiyarasu, R. and Somayaji, K.M. (2002). A Study of Atmospheric Dispersion of Radionucleides at a Coastal Site Using a Modified Gaussian Model and a Meso-scale Sea Breeze Model. *Atmos. Environ.* 36: 2933–2942.

Viana, M., Perez, C., Querol, X., Alastuey, A., Nickovic, S. and Baldasano, J.M. (2005). Spatial and Temporal Variability of PM Levels and Composition in a Complex Summer Atmospheric Scenario in Bacrcelona (NE Spain). *Atmos. Environ.* 39: 5343–5361.

Yang, K.L. (2002). Spatial and Seasonal Variation of PM_{10} Mass Concentrations in Taiwan. *Atmos. Environ.* 36: 3403–3411.

Yu, T.I. and Chang, L.F.W. (2000). Selection of the Scenarios of Ozone Pollution at Southern Taiwan Area Utilizing Principal Component Analysis. *Atmos. Environ.* 34: 4499–4509.

Yuan, C.S., Lee, C.G., Liu, S.H., Chang, J.C., Yuan C. and Yang, H.Y. (2006). Correlation of Atmospheric Visibility with Chemical Composition of Kaohsiung Aerosols. *Atmos. Res.* 82: 663–679.

Yuan, C.S., Sau, C.C., Chen, M.C., Hung, M.H., Chang, S.W. and Lin, Y.C. (2004). Mass Concentration and Size-resolved Chemical Composition of Atmospheric Aerosols Sampled at Pescardores Islands during Asian Dust Storm periods in the Years of 2001 and 2002. *Terr. Atmos. Ocean. Sci.* 15: 857–879.

Received for review, December 30, 2010
Accepted, April 29, 2011